

Electronic Supplementary Information (ESI) for

Synthesis of ultrasmall CsPbBr₃ nanoclusters and their transformation to highly deep-blue-emitting nanoribbons at room temperature

Yibing Xu,^a Qiang Zhang,^a Longfei Lv,^b Wenqian Han,^a Guanhong Wu,^a Dong Yang,^b and Angang Dong ^{*a}

^aCollaborative Innovation Center of Chemistry for Energy Materials, Shanghai Key Laboratory of Molecular Catalysis and Innovative Materials, and Department of Chemistry, Fudan University, Shanghai 200433, China.

^bState Key Laboratory of Molecular Engineering of Polymers, Collaborative Innovation Center of Polymers and Polymer Composite Materials, and Department of Macromolecular Science, Fudan University, Shanghai 200433, China.

*To whom correspondence should be addressed: agdong@fudan.edu.cn (A.D.)

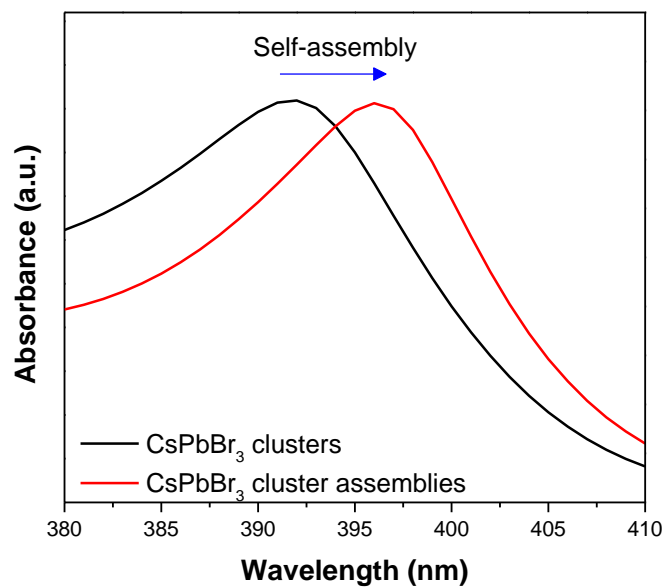


Fig. S1. The first absorption peak of CsPbBr₃ nanoclusters and their assemblies, respectively, showing a ~ 7 nm red-shift along with the cluster assembly.

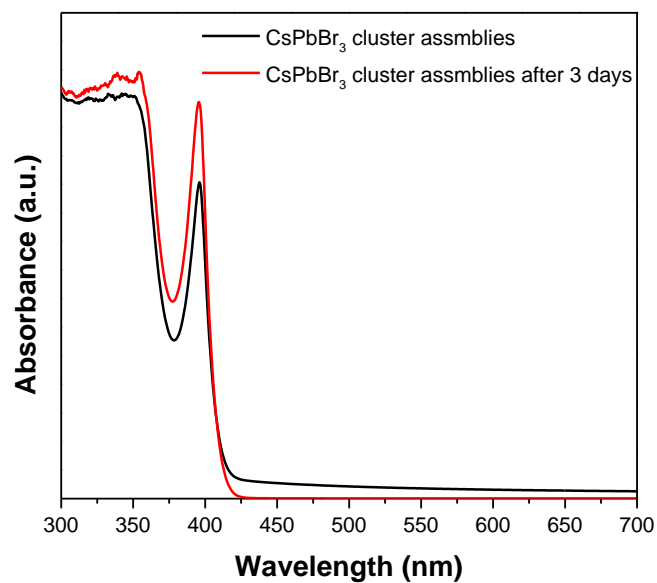


Fig. S2. Absorption spectra of the as-formed CsPbBr₃ cluster assemblies and those after 3 days of storage in air. The essentially unchanged absorption spectrum upon prolonged exposure to air indicated the high chemical stability of CsPbBr₃ cluster ensembles.

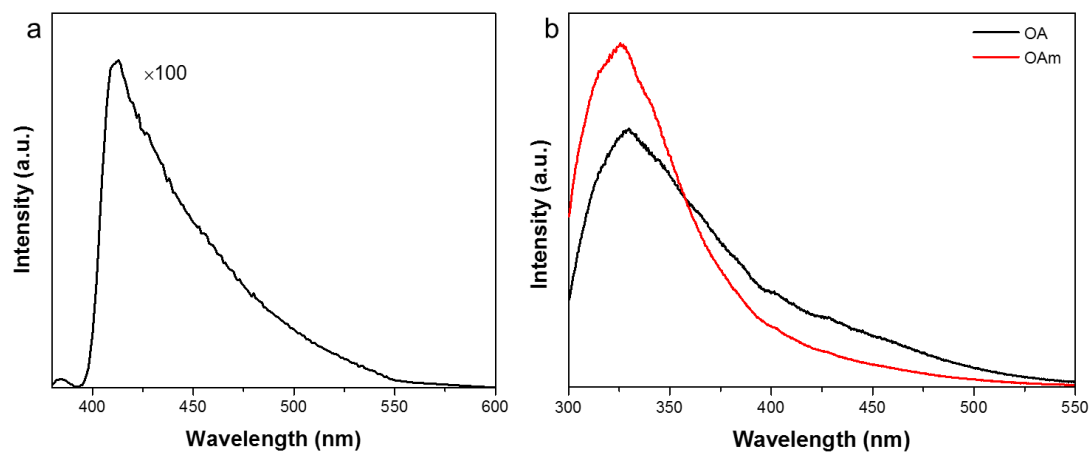


Fig. S3. (a) PL spectrum of CsPbBr₃ cluster assemblies, showing a broad PL peak near 410 nm. (b) PL spectra of OA and OAm ligands

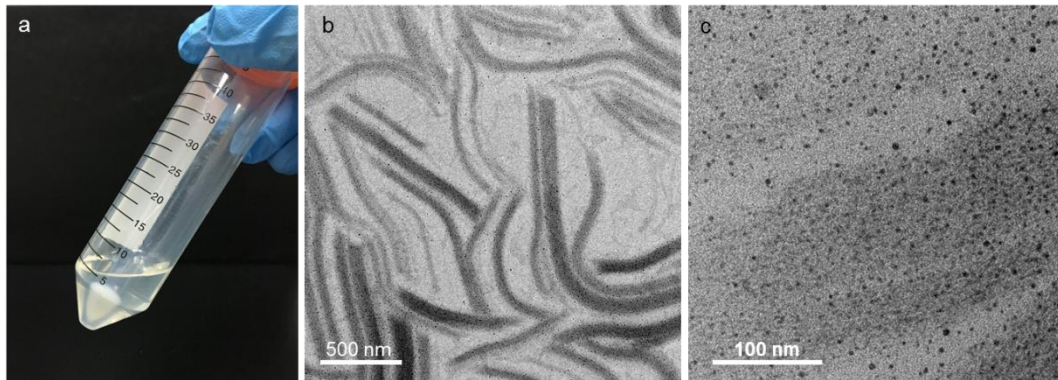


Fig. S4. (a) Photograph of a CsPbBr₃ nanocluster solution after centrifugation, showing the white cluster precipitates. (b) Low-magnification TEM image of CsPbBr₃ cluster assemblies. (c) Magnified TEM image of the cluster assemblies, showing the parallel fringe patterns. The black dots in (c) are expected to be Pb nanoparticles formed upon prolonged electron-beam exposure. Similar dark dots, originating from the reduction of Pb²⁺ by the electron beam, have been commonly observed in TEM on CsPbBr₃ nanosheets or nanocrystals.

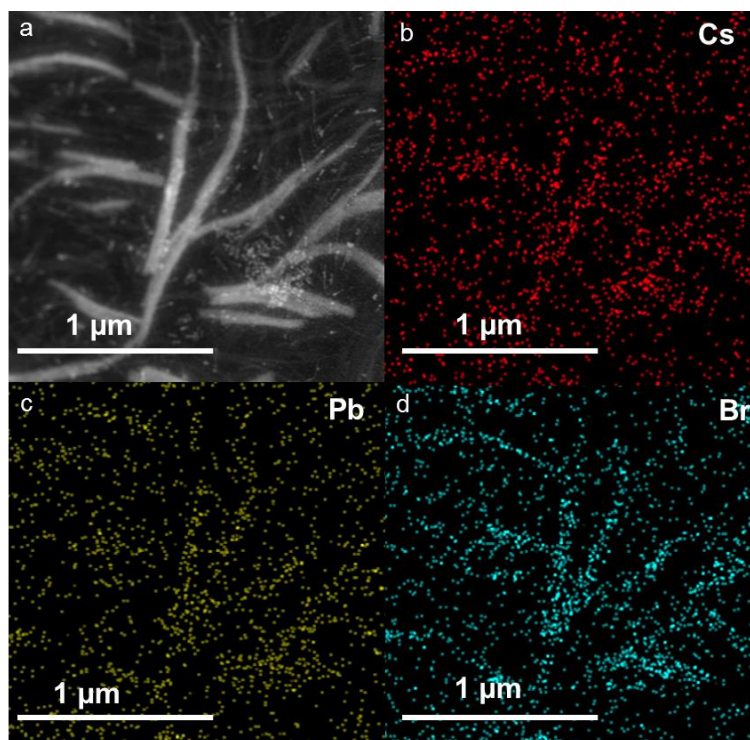


Fig. S5. (a) Dark-field STEM image of CsPbBr₃ cluster assemblies and (b-d) the corresponding elemental mapping images, showing the existence of Cs, Pb, and Br within the cluster assemblies.

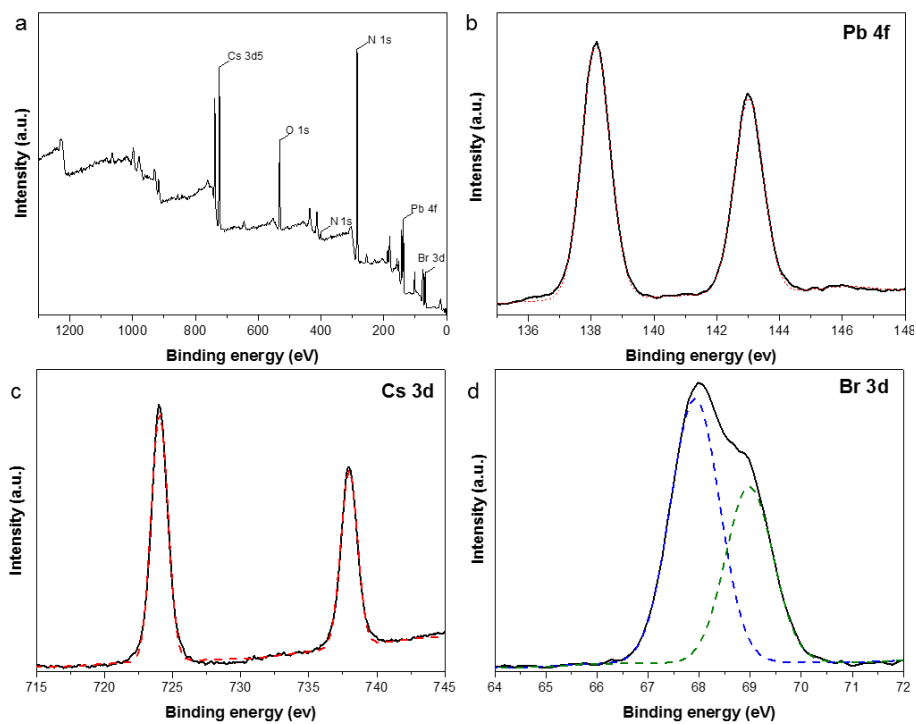


Fig. S6. (a) XPS spectrum and the Pb 4f (b), Cs 3d (c), and Br 3d (d) spectral profiles of CsPbBr₃ cluster assemblies. The solid lines are the experimental data and the dotted lines are the fits. The atomic ratio of Cs/Pb/Br was determined to be 0.9:0.9:3.0.

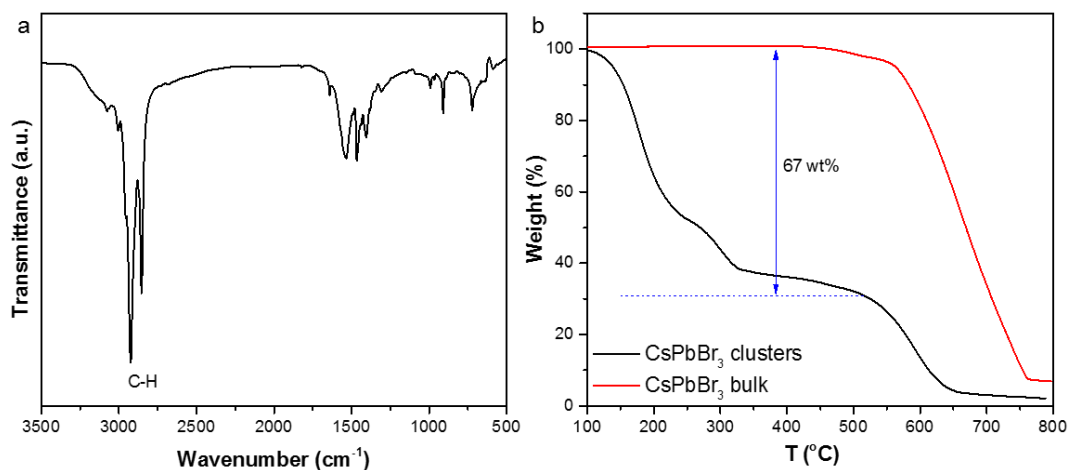


Fig. S7. (a) FTIR spectrum of CsPbBr₃ cluster assemblies, showing the presence of a large amount of OA/OAm ligands as indicated by the strong C-H stretching bands near 2900 cm⁻¹. (b) TGA curves of CsPbBr₃ cluster assemblies (black curve) and CsPbBr₃ bulk materials (red curve) conducted in air. The weight loss of CsPbBr₃ cluster assemblies before 500 °C was attributed to the thermally decomposed organic ligands, whereas the weight loss after 500 °C was probably caused by the decomposition of CsPbBr₃, as indicated by the bulk curve.

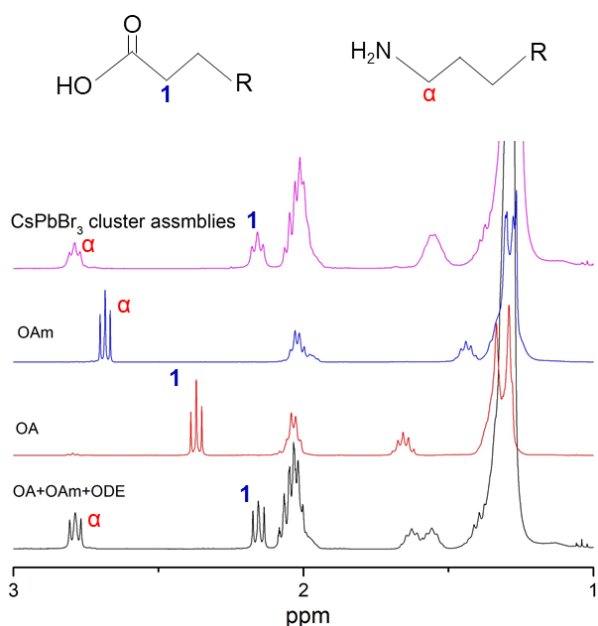


Fig. S8. ^1H NMR spectroscopic analysis of the isolated CsPbBr_3 cluster assemblies. The reference spectra of OA and OAm as well as OA/OAm in ODE were also provided for comparison. The organic residues derived from CsPbBr_3 cluster assemblies exhibited the characteristic resonances of **1** and α , corresponding to OA and OAm, respectively, in the ^1H NMR spectra, corroborating the presence of both OA and OAm ligands. Note that both characteristic resonances of **1** and α were slightly shifted compared with those of OA and OAm reference spectra, which was presumably caused by the reaction between OA and OAm. This was further confirmed by collecting the NMR spectrum of an OA and OAm mixture in ODE, where the characteristic resonances of **1** and α matched well with those of CsPbBr_3 cluster assemblies.

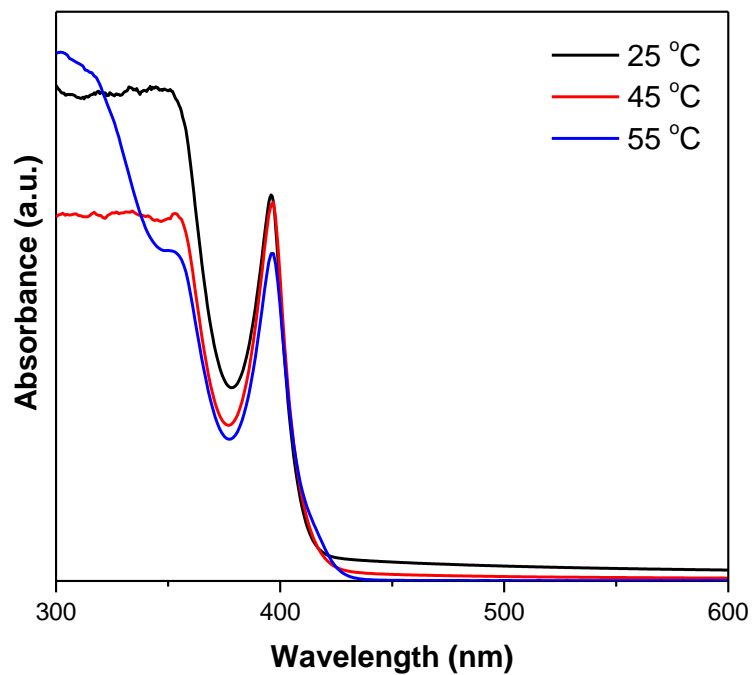


Fig. S9. Absorption spectra of CsPbBr₃ cluster assemblies synthesized under different reaction temperatures. The characteristic absorption peak at ~398 nm suggested the formation of the same sized clusters irrespective of the reaction temperature.

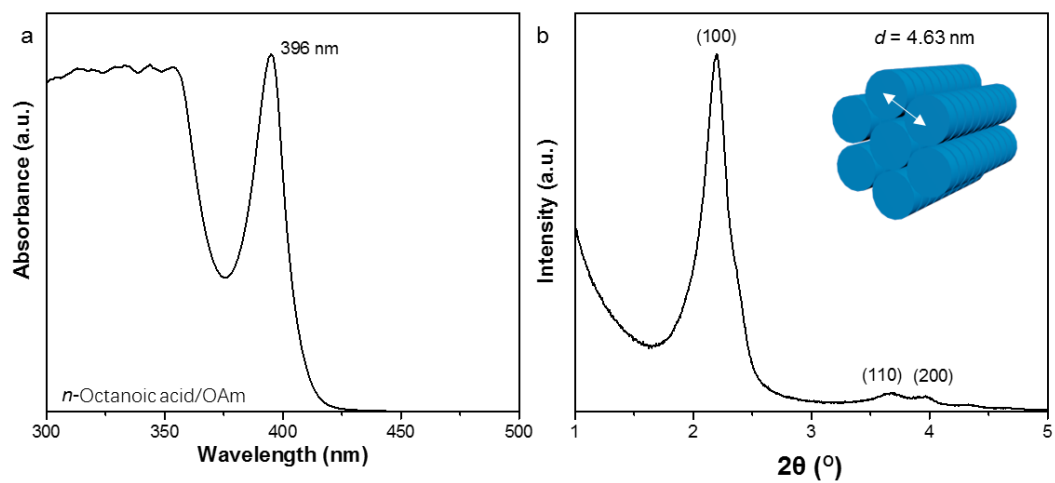


Fig. S10. (a) Absorption spectra and (b) small-angle XRD pattern of CsPbBr₃ cluster assemblies synthesized with the ligands of *n*-octanoic acid/OAm.

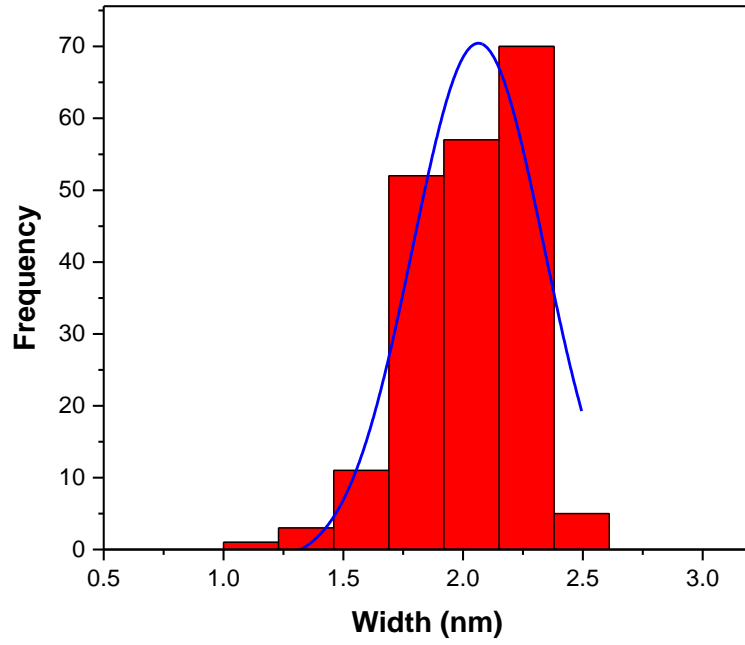


Fig. S11. Width distribution histogram of CsPbBr₃ quantum nanoribbons, showing that the average width was 2.2 nm.

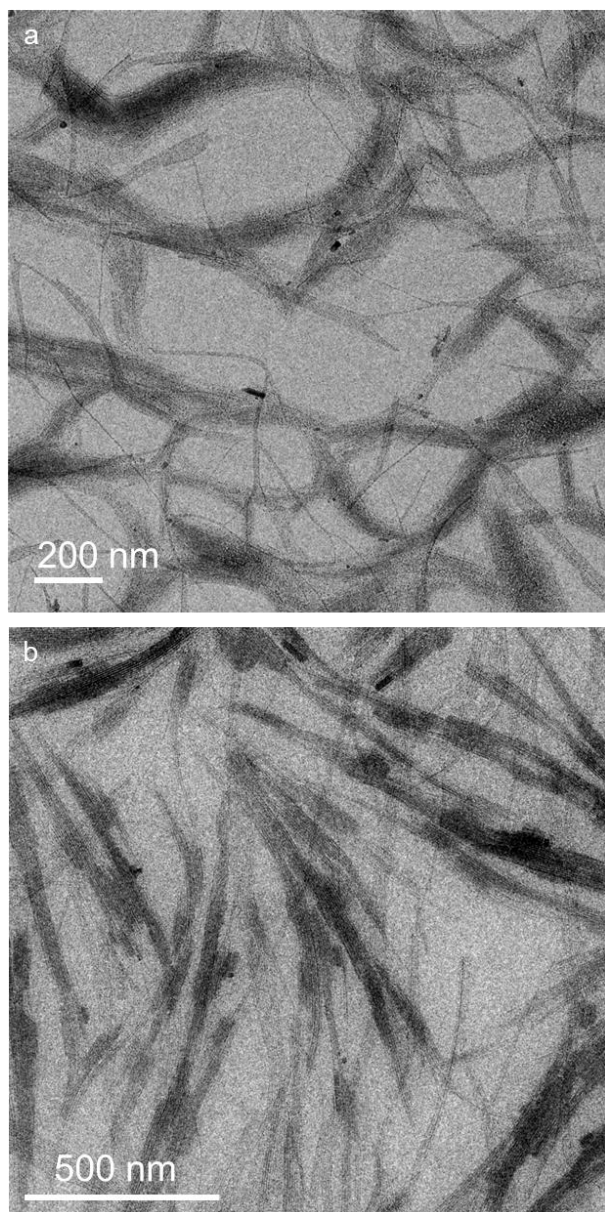


Fig. S12. (a, b) Low-magnification TEM images of CsPbBr₃ nanoribbon bundles.

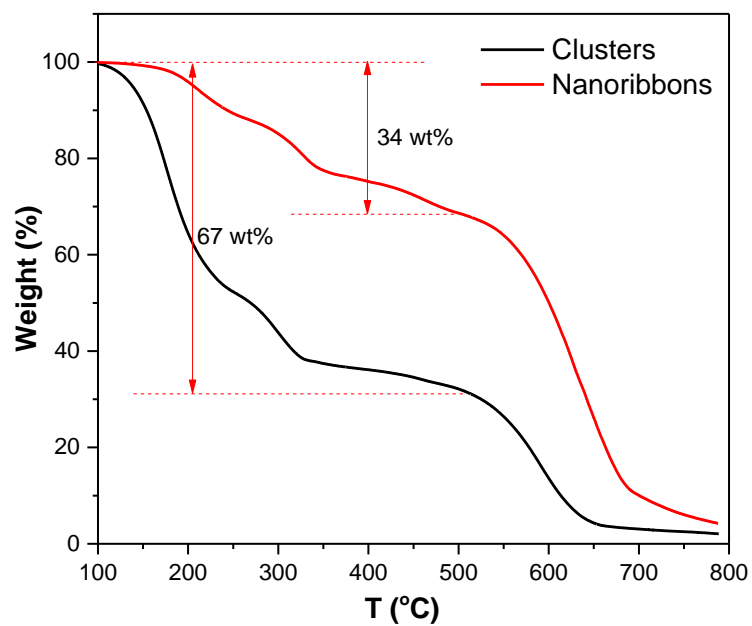


Fig. S13. TGA curves of CsPbBr₃ cluster assemblies (black curve) and nanoribbons (red curve), showing the significant loss of organic ligands along with the transformation of CsPbBr₃ nanoclusters.